*Inorg. Chem.* **2005**, *44*, 4630–4636

Inorganic Chemistry

Article

# Enantiomerically Pure Pentagonal-Bipyramidal Metal Complexes with Predetermined Helicity in the Solid and Solution States

**Michael Seitz,[†] Anja Kaiser,[†] Sabine Stempfhuber,[‡] Manfred Zabel,[‡] and Oliver Reiser*,[†]**

*Institute for Organic Chemistry, University of Regensburg, Universitätsstrasse 31,*
*D-93053 Regensburg, Germany*

Received January 5, 2005

New metal complexes with pentagonal-bipyramidal geometry have been synthesized with the chiral, pentadentate bis(oxazoline) ligand (*R*,*R*)-**1**, including the metal ions magnesium(II), iron(II), and cadmium(II). In the solid state, a complete transfer of chirality from the ligand is observed to exclusively yield enantiomerically pure *P*-helical, isostructural pentagonal bipyramidal complexes, as determined by X-ray analysis of four compounds. This uncommon coordination geometry is likely to be driven by $\pi$–$\pi$-stacking of the terminal phenyl groups of the linear ligands. The complex cations in $[Fe((R,R)\text{-}\mathbf{1})(H_2O)_2](ClO_4)_2$ (**3**), $[Cd((R,R)\text{-}\mathbf{1})(H_2O)_2](ClO_4)_2$ (**4**), and $[Mg((R,R)\text{-}\mathbf{1})(H_2O)_2](ClO_4)_2$ (**5**) are mononuclear with the two apical positions of the pentagonal bipyramide occupied by two water molecules. In contrast, the structure in dinuclear $[Cd((R,R)\text{-}\mathbf{1})(MeOH)(\mu\text{-}I)(CdI_3)]$ (**2c**) can be described as pentagonal-bipyramidal around cadmium with MeOH and distorted-tetrahedral $CdI_4$ (via one bridging iodo ligand) completing the coordination sphere in axial positions. The crystal packing of **3**–**5** shows a highly ordered orientation of the mononuclear helical cations into one-dimensional chains along the crystallographic axis *a*, stabilized by intermolecular $\pi$–$\pi$-stacking. In contrast, the dinuclear helices in **2c** are tilted relative to one another, and consequently, directed, one-dimensional helicity in the solid state is not observed. Studies using a combination of mass spectrometry and NMR and CD spectroscopy indicate the presence of only one $C_2$-symmetrical, mononuclear species in acetonitrile for each case, suggesting the formation of diastereo- and enantiomerically pure complexes also in the solution state. All compounds exhibit a very characteristic and almost identical CD pattern between 200 nm and 300 nm. This signal can be attributed to the *P*-helical, pentagonal arrangement of the ligand.

## Introduction

Metal complexes with coordination number 7 are rather rare,[1] especially with first-row transition metals.[2] In most cases, such species adopt a pentagonal-bipyramid. This coordination geometry can be enforced by rigid pentadentate ligands that have a strong tendency for coplanar arrangement of the five donor atoms, leaving the two apical positions open for monodentate external ligands. Realization of this positional preference is normally achieved by the employment of linear, resonance-stabilized ligands as found with imine-type derivatives of 2,6-diacetylpyridine[3] or by the incorporation of the chelating units into a macrocyclic system such as in 15-crown-5[4] or related ligands.[5]

The construction of helical metal–ligand assemblies is an active research area with great impact on important fields such as supramolecular chemistry,[6] asymmetric catalysis,[7]

---

* Author to whom correspondence should be addressed. E-mail: oliver.reiser@chemie.uni-regensburg.de. Phone: +49-941-943-4631. Fax: +49-941-943-4121.

[†] Institute of Organic Chemistry, University of Regensburg.

[‡] Crystallography Laboratory, University of Regensburg.

(1) According to the following reference, heptacoordinate complexes represent only 1.8% of all $\sigma$-bonded transition metal complexes reported in the Cambridge Structural Database: Casanova, D.; Alemany, P.; Bofill, J. M.; Alvarez, S. *Chem.—Eur. J.* **2003**, *9*, 1281–1295.

(2) (a) Drew, M. G. B. *Prog. Inorg. Chem.* **1977**, *23*, 67–210. (b) Kepert, D. L. *Prog. Inorg. Chem.* **1979**, *25*, 41–144. (c) Melnik, M.; Sharrock, P. *Coord. Chem. Rev.* **1985**, *65*, 49–85.

(3) Review: Ivanovic-Burmazovic, I.; Andjelkovic, K. *Adv. Inorg. Chem.* **2004**, *55*, 315–360.

(4) Selected recent examples: (a) Sanchez, E. R.; Gessel, M. C.; Groy, T. L.; Caudle, M. T. *J. Am. Chem. Soc.* **2002**, *124*, 1933–1940. (b) Atwood, J. L.; Junk, P. C. *Polyhedron* **2000**, *19*, 85–91.

(5) Some recent examples: (a) Patroniak, V.; Kubicki, M.; Mondry, A.; Lisowski, J.; Radecka-Paryzek, W. *J. Chem. Soc., Dalton Trans.* **2004**, 3295–3304. (b) Korendovych, I. V.; Staples, R. J.; Reiff, W. M.; Rybak-Akimova, E. V. *Inorg. Chem.* **2004**, *43*, 3930–3941. (c) Marquez, V. E.; Anacona, J. R.; Lorono, D. *Polyhedron* **2004**, *23*, 1317–1323. (d) Keypour, H.; Khanmohammadi, H.; Wainwright, K. P.; Taylor, M. R. *Inorg. Chim. Acta* **2003**, *355*, 286–291. (e) Madalan, A. M.; Voronkova, V.; Galeev, R.; Korobchenko, L.; Magull, J.; Roesky, H. W.; Andruh, M. *Eur. J. Inorg. Chem.* **2003**, 1995–1999.

10.1021/ic050014b CCC: $30.25

© 2005 American Chemical Society
Published on Web 05/27/2005

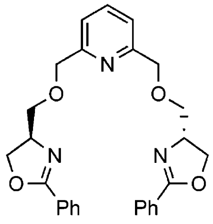

(*R*,*R*)-**1**

**Figure 1.** Pentadentate bis(oxazoline) ligand (*R*,*R*)-**1**.

nonlinear optical applications,[8] or molecular recognition.[9] Pentagonal-bipyramidal metal complexes with achiral ligands of this kind are normally inherently achiral because of the planarity of the ligand arrangement.[10] However, if certain parts of the ligand backbone deviate from the pentagonal plane, the resulting helical structure introduces a source of chirality. Only a few examples for this phenomenon are known for pentagonal-bipyramidal systems with linear, pentadentate ligands, albeit to the best of our knowledge only as racemic mixtures.[11]

We recently reported the new chiral pentadentate bis(oxazoline) ligand (*R*,*R*)-**1** (Figure 1) that forms one-dimensional inorganic−organic hybrid polymers with unprecedented design in the solid state with $CdCl_2$ and $CdBr_2$,[12a] as well as mononuclear, trigonal-bipyramidal zinc complexes.[12b] In both cases, complete predetermination of helical chirality around the metal center could be achieved.

Herein, we report new representatives of enantiomerically pure, helical complexes with pentagonal-bipyramidal geometry. These species include a halogen-bridged dinuclear compound with the previously unstudied cadmium halide $CdI_2$. In addition, for the first time mononuclear complexes of the above-mentioned kind are identified and characterized, both in the solid state and in solution.

## Results and Discussion

**Complex Synthesis.** To test whether the design principle of the polymeric species **2a**,**b** (Scheme 1) could be extended to cadmium halides other than $CdCl_2$ and $CdBr_2$, a new complex with $CdI_2$ was synthesized to complete the series of Cl, Br, and I. The preparation was achieved in the same way as for **2a**,**b** by refluxing (*R*,*R*)-**1** and the cadmium iodide in methanol. Upon cooling, the complex was separated by filtration and dried in vacuo to give the analytically pure compound **2c** in excellent yields.

The behavior of the iodide containing complex **2c** is markedly different from that of the polymeric species **2a**,**b**. In contrast to the latter, **2c** melts at a considerably lower temperature (**2a**,**b**, >200 °C; **2c**, 131−137 °C) and the solubility in organic solvents is greatly improved, indicative for a nonpolymeric structure.

For the synthesis of the perchlorate complexes **3**−**5**, equimolar amounts of metal perchlorates and ligand (*R*,*R*)-**1** were dissolved separately in dry THF under dinitrogen (Scheme 2), and the precipitating complexes were isolated by filtration and dried in vacuo.

The low yield in which the Fe(II) complex **3** was obtained is probably due to its oxidative degradation to Fe(III); nevertheless, **3** could be isolated in analytically pure form. Unfortunately, no sufficient elemental analysis could be obtained for the Cd(II) and Mg(II) species because these complexes are subject to strongly disordered inclusion of solvent molecules into the crystal lattice (vide infra). The yield for **4** and **5** exceeds 80%, estimated by a simple mass balance (see Experimental Section).

**Solid-State Structures.** Crystals suitable for X-ray analysis could be obtained for compounds **2c** (recrystallization from MeOH), **3** and **4** (vapor diffusion of $Et_2O$ into $CH_3CN$ solutions), and **5** (vapor diffusion of $Et_2O$ into acetone solution). While **2c** ($R = 0.0295$) and **3** ($R = 0.044$) were unproblematic, the structures of **4** and **5** could not completely be solved to R-values $< 0.05$ (**4**, 0.094; **5**, 0.061) due to the disordering of solvent molecules mentioned above. Nevertheless, the positions of the complex cations and the perchlorate anions could be easily refined and the complex structures unambiguously assigned. They show essentially the same geometry as for **3**.

**2c** exhibits a dinuclear nature, where one cadmium cation has pentagonal-bipyramidal geometry with (*R*,*R*)-**1** residing in the pentagonal plane. The coordination sphere in axial position is completed by MeOH and a distorted tetrahedral $CdI_4$ unit via one bridging iodide (Figure 2, Table 1).[13] Like in **2a**,**b**, ligand (*R*,*R*)-**1** wraps around the metal center in a helical fashion, exclusively yielding right-handed helicity.

Several seven-coordinate cadmium species with pentagonal-bipyramidal coordination geometry have been reported.[11c,d,14] The structure of **2c** resembles the previously reported binuclear compound $[Cd(15\text{-crown-}5)(MeOH)(\mu\text{-Br})CdBr_3)]$;[15] however, due to the chirality of the ligand *P*-helicity is induced.

Likewise, the mononuclear complex cations in **3**−**5** have a similar heptacoordinate structure: (*R*,*R*)-**1** folds again with

---

[6] (a) Piguet, C.; Bernardinelli, G.; Hopfgartner, G. *Chem. Rev.* **1997**, *97*, 2005−2062. (b) Albrecht, M. *Chem. Rev.* **2001**, *101*, 3457−3497. (c) Hannon, M. J.; Childs, L. *J. Supramol. Chem.* **2004**, *16*, 7−22.

[7] Review: *Comprehensive Asymmetric Catalysis*; Jacobsen, E. N., Pfaltz, A., Yamamoto, H., Eds.; Springer: Berlin, 1999; Vols. 1−3.

[8] Review: Evans, O. R.; Lin, W. *Acc. Chem. Res.* **2002**, *35*, 511−522 and references cited therein.

[9] Selected recent examples: (a) Kano, K.; Hasegawa, H. *J. Am. Chem. Soc.* **2001**, *123*, 10616−10627; (b) Fiedler, D.; Leung, D. H.; Bergman, R. G.; Raymond, K. N. *J. Am. Chem. Soc.* **2004**, *126*, 3674−3675.

[10] Von Zelewsky, A. *Stereochemistry of Coordination Compounds*; Wiley: Chichester, U.K., 1996.

[11] (a) Chessa, G.; Marangoni, G.; Pitteri, B.; Bertolasi, V.; Ferretti, V.; Gilli, G. *J. Chem. Soc., Dalton. Trans.* **1988**, 1479−1485. (b) Constable, E. C.; Walker, J. V.; Tocher, D. A.; Daniels, M. A. M *Chem. Commun.* **1992**, 768−771. (c) Beynek, N.; McPartlin, M.; Murphy, B. P.; Scowen I. J. *Polyhedron* **1998**, *17*, 2137−2140. (d) Pedrido, R.; Bermejo, M. R.; García-Deibe, A. M.; González-Noya, A. M.; Maneiro, M.; Vázquez, M. *Eur. J. Inorg. Chem.* **2003**, 3193−3200.

[12] (a) Seitz, M.; Kaiser, A.; Stempfhuber, S.; Zabel, M.; Reiser, O. *J. Am. Chem. Soc.* **2004**, *126*, 11426−11427. (b) Seitz, M.; Stempfhuber, S.; Zabel, M.; Schütz, M.; Reiser, O. *Angew. Chem., Int. Ed.* **2005**, *44*, 245.

[13] For a more detailed description, see the Supporting Information.

[14] Selected recent examples with linear, pentadentate ligands: (a) Fondo, M.; Sousa, A.; Bermejo, M. R.; García-Deibe, A.; Sousa-Pedrares, A.; Hoyos, O. L.; Helliwell, M. *Eur. J. Inorg. Chem.* **2002**, 703−710. (b) Loukiala, S.; Ratilainen, J.; Airola, K.; Valkonen, J.; Rissanen, K. *Acta Chem. Scand.* **1998**, *52*, 593−602.

[15] Rogers, R. D.; Bond, A. H. *Inorg. Chim. Acta* **1996**, *250*, 105−117.

**Scheme 1.** Coordination Compounds of (*R*,*R*)-**1** with Cadmium Halides

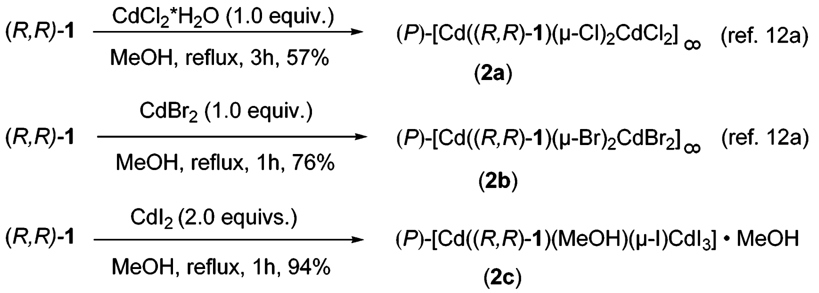

**Scheme 2.** Metal Complexes of (*R*,*R*)-**1** with Noncoordinating Perchlorate Anions

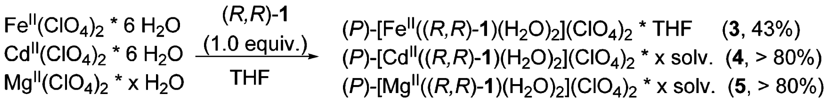

*P*-helicity around the pentagonal coordinated metal, and two water molecules complete the pentagonal bipyramid in apical positions (Figures 3−5).

Bond lengths and angles in all four crystal structures are in the normal range and display no unusual features (Tables 2 and 3).[13] The nature of the pentagonal-bipyramidal geometry is almost identical in all complexes **2a**−**c** and **3**−**5**. In **2c**, **3**, and **4**, only one unique unit is present, whereas in **5** two unique but only marginally differing cations exist. The pentagonal-bipyramidal coordination mode for the cadmium complex **4** is not unusual.[14] In contrast, this geometry is rather rare for iron(II)[4b,16] and magnesium(II),[4a,17] especially with topologically linear ligands such as (*R*,*R*)-**1**.

Since the linear ligand (*R*,*R*)-**1** is not obviously set up for coplanar arrangement of the five donor atoms due to its flexible backbone consisting of a considerable number of sp$^3$-hybridized atoms, the observation of this unusual mode of coordination is striking. Although the oxazoline units are already slightly tilted to induce helicity, the driving force for the formation of the helical, heptacoordinate complexes is likely to be the $\pi-\pi$-stacking of the two phenyl moieties (Figure 6), and work in our laboratories is ongoing to synthesize ligands in which the phenyl groups are exchanged by alkyl groups to corroborate this hypothesis. In all four cases, the phenyl moieties have a laterally displaced, almost parallel orientation to each other with a distance of ca. 3.4−3.5 Å. This is within the normal range of 3.3−3.6 Å for interactions of this kind.[18]

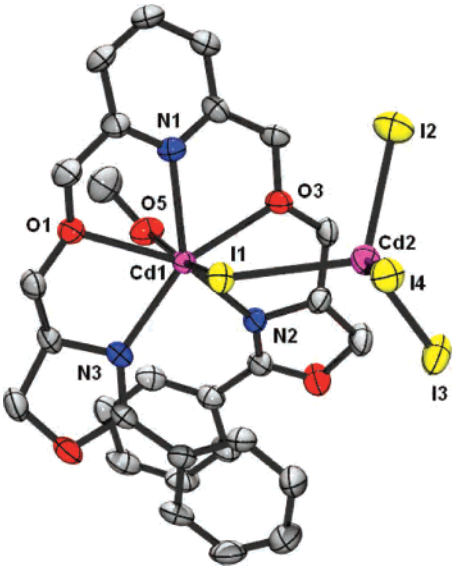

**Figure 2.** Thermal ellipsoid plot for the asymmetric units of **2c**: [Cd((*R*,*R*)-**1**)(MeOH)($\mu$-I)CdI$_3$)] (50% probability level, hydrogens omitted, with atom numbering scheme).

The packing of the individual complexes **3**−**5** in the solid state also has some interesting features, showing one-dimensional, columnar stacking of the cations along the crystallographic axis *a*, thereby resulting in one-dimensional strands of overall right-handed helicity (Figure 7).

This overall assembly is again likely to be stabilized by $\pi-\pi$-stacking interactions of the phenyl rings, both intra- and intermolecular (distance between aromatic phenyl planes ca. 3.4 Å), and resembles the one-dimensional chains in covalently linked polymers **2a**,**b**.[12a] The arrangement of the columns relative to one another is different for **3** and **4** and **5**, the latter pair having the same structure (Figure 8). This phenomenon probably also accounts for the different incorporation of solvent molecules into the crystal lattice (vide supra).

The packing for the complex **2c** is the only example reported here where the complexes are not stacked in a parallel fashion to give the columnar structure. Instead, the dinuclear units are tilted and shifted relative to each neighbor unit, which results in the loss of the highly ordered, one-dimensional helical array discussed above (Figure 9).

**Solution-State Structures.** Generally, pentagonal-bipyramidal metal complexes are identified and characterized almost exclusively by means of X-ray analysis. In solution,

---

(16) Selected recent examples: (a) Galán-Mascarós, J.-R.; Clemente-Juan, J.-M.; Dunbar, K. R. *J. Chem. Soc., Dalton Trans.* **2002**, 2710−2713. (b) Hayami, S.; Gu, Z.-z.; Einaga, Y.; Kobayasi, Y.; Ishikawa, Y.; Yamada, Y.; Fujishima, A.; Sato, O. *Inorg. Chem.* **2001**, *40*, 3240−3242. (c) Lainé, P.; Gourdon, A.; Launay, J.-P.; Tuchagues, J.-P. *Inorg. Chem.* **1995**, *34*, 5150−5155 and references cited therein.

(17) Selected recent examples: (a) Keypour, H.; Khanmohammadi, H.; Wainwright, K. P.; Taylor, M. R. *Inorg. Chim. Acta* **2004**, *357*, 1283−1291. (b) Park, K. M.; Yoon, I.; Seo, J.; Lee, Y. H.; Lee, S. S. *Acta Crystallogr., Sect. E: Struct. Rep. Online* **2001**, *E57*, m154−m156. (c) Li, Y.; Yamauchi, J.; Azuma, N. *J. Coord. Chem.* **1997**, *42*, 291−302.

(18) (a) Dahl, T. *Acta Chem. Scand.* **1994**, *48*, 96−106. (b) Janiak, C. *J. Chem. Soc., Dalton Trans.* **2000**, 3885−3896.

**Table 1.** X-ray Crystallographic Data Collection and Refinement Details for **2c** and **3**−**5**[11]

| param | [Fe((*R*,*R*)-**1**)($H_2O$)$_2$](ClO$_4$)$_2$·THF (**3**) | [Cd((*R*,*R*)-**1**)($H_2O$)$_2$](ClO$_4$)$_2$·*x* solv (**4**) | [Mg((*R*,*R*)-**1**)($H_2O$)$_2$](ClO$_4$)$_2$·*x* solv (**5**) | [Cd((*R*,*R*)-**1**)(MeOH)($\mu$-I)CdI$_3$]·MeOH (**2c**) |
|---|---|---|---|---|
| formula | $C_{31}H_{39}Cl_2FeN_3O_{15}$ | $C_{27}H_{31}CdCl_2N_3O_{14}$·*x* solv | $C_{27}H_{31}Cl_2MgN_3O_{14}$·*x* solv | $C_{29}H_{35}Cd_2I_4N_3O_6$ |
| mol wt | 820.40 | 804.86 + *x* solv | 716.76 + *x* solv | 1254.04 |
| cryst system | orthorhombic | monoclinic | monoclinic | monoclinic |
| space group | $P2_12_12_1$ | $P2_1$ | $P2_1$ | $P2_1$ |
| $a$ (Å) | 8.2616(7) | 8.6140(13) | 8.6129(8) | 12.1883(13) |
| $b$ (Å) | 14.0004(10) | 19.322(2) | 19.3622(11) | 13.5960(10) |
| $c$ (Å) | 30.790(2) | 10.8199(19) | 20.792(2) | 12.9392(13) |
| α (deg) | 90 | 90 | 90 | 90 |
| $\beta$ (deg) | 90 | 107.088(19) | 96.846(11) | 115.881(11) |
| $\gamma$ (deg) | 90 | 90 | 90 | 90 |
| $V$ (Å$^3$) | 3561.3(5) | 1721.4(5) | 3442.7(5) | 1929.1(4) |
| $Z$ | 4 | 2 | 4 | 2 |
| $\rho$ (g cm$^{-3}$) | 1.530 | 1.545 | 1.418 | 2.145 |
| radiatn (Å) | Mo Kα ($\lambda$ = 0.710 73) | Mo Kα ($\lambda$ = 0.710 73) | Mo Kα ($\lambda$ = 0.710 73) | Mo Kα ($\lambda$ = 0.710 73) |
| $\mu$(Mo Kα) (mm$^{-1}$) | 0.648 | 0.857 | 0.279 | 4.342 |
| temp (K) | 173(1) | 173(1) | 173(1) | 173(1) |
| R$^a$ ($I \geq 2\sigma(I)$) | 0.0443 | 0.0937 | 0.0605 | 0.0295 |
| wR$_2^b$ ($I \geq 2\sigma(I)$) | 0.0884 | 0.2477 | 0.1209 | 0.0764 |
| absolute struct param | −0.01(2) | 0.13(7) | 0.16(8) | 0.00(2) |

[a] R factor definition: $R = \Sigma(||F_o| - |F_c||)/\Sigma|F_o|$. [b] SHELX-97 wR$_2$ factor definition: $wR_2 = [\Sigma w(F_o^2 - F_c^2)^2/\Sigma w(F_o^4)]^{1/2}$. Weighting scheme: $w = 1/[\sigma^2(F_o)^2 + (np)^2]$, $p = [F_o^2 + 2F_c^2]/3$.

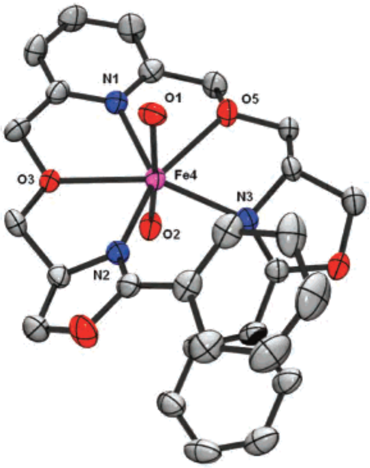

**Figure 3.** Thermal ellipsoid plot for the asymmetric units of **3**: [Fe((*R*,*R*)-**1**)($H_2O$)$_2$]$^{2+}$ (50% probability level, hydrogens omitted, with atom numbering scheme).

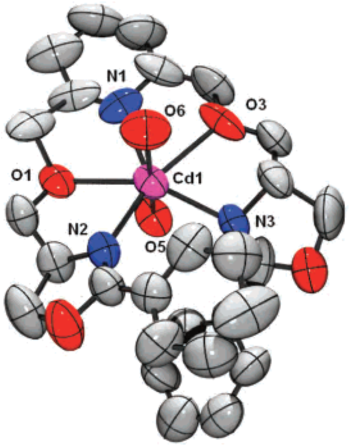

**Figure 4.** Thermal ellipsoid plot for the asymmetric units of **4**: [Cd((*R*,*R*)-**1**)($H_2O$)$_2$]$^{2+}$ (50% probability level, hydrogens omitted, with atom numbering scheme).

only very few studies have been carried out regarding this coordination geometry, mostly dealing with substitution behavior.[19] The compounds **2**−**5** dissolve in polar solvents such as $CH_3CN$, MeOH, or acetone, albeit only poorly for the polymeric species **2a**,**b**. In DMF and DMSO, the complex

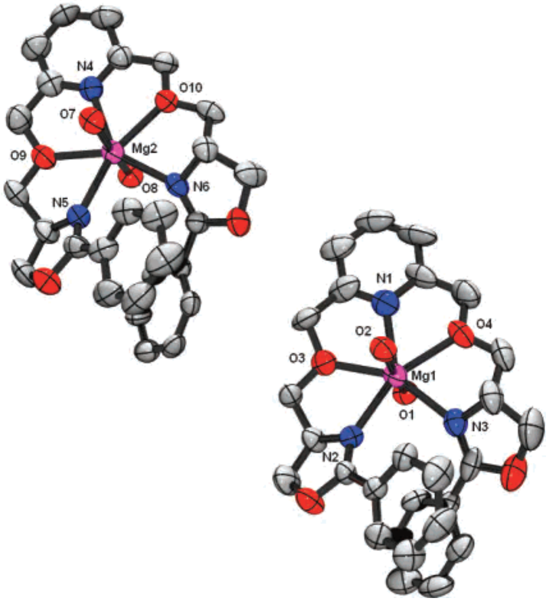

**Figure 5.** Thermal ellipsoid plot for the two unique units of **5**: [Mg((*R*,*R*)-**1**)($H_2O$)$_2$]$^{2+}$ (50% probability level, hydrogens omitted, with atom numbering scheme).

**Table 2.** Selected Bond Lengths (Å) in Complexes **2c** and **3**−**5**$^a$

| | **2c** (M = Cd) | **3** (M = Fe) | **4** (M = Cd) | **5A**$^b$ (M = Mg) | **5B**$^b$ (M = Mg) |
|---|---|---|---|---|---|
| M−N$_{\text{pyridine}}$ | 2.395(5) | 2.339(1) | 2.356(15) | 2.326(6) | 2.327(6) |
| M−N$_{\text{oxazoline1}}$ | 2.396(6) | 2.268(3) | 2.350(15) | 2.310(7) | 2.361(6) |
| M−N$_{\text{oxazoline2}}$ | 2.371(5) | 2.232(3) | 2.348(12) | 2.305(6) | 2.296(7) |
| M−O$_{\text{ether1}}$ | 2.506(5) | 2.336(3) | 2.455(10) | 2.292(5) | 2.261(5) |
| M−O$_{\text{ether2}}$ | 2.412(4) | 2.332(3) | 2.413(10) | 2.274(5) | 2.239(5) |
| M−X$_{\text{axial1}}$ | 2.9719(7)$^c$ | 2.148(3)$^d$ | 2.325(11)$^d$ | 2.062(5)$^d$ | 2.072(4)$^d$ |
| M−X$_{\text{axial2}}$ | 2.400(5)$^c$ | 2.111(3)$^d$ | 2.303(9)$^d$ | 2.055(4)$^d$ | 2.054(5)$^d$ |

[a] Estimated standard deviations are given in parentheses. [b] Two independent cations in the asymmetric unit. [c] X$_{\text{axial1}}$ = I, X$_{\text{axial2}}$ = O$_{\text{MeOH}}$. [d] X$_{\text{axial1}}$ = O$_{\text{water1}}$, X$_{\text{axial2}}$ = O$_{\text{water2}}$.

---

(19) Ivanovic-Burmazovic, I.; Hamza, M. S. A.; Van Eldik, R. *Inorg. Chem.* **2002**, *41*, 5150−5161 and references cited therein.

**Table 3.** Selected Bond Angles (deg) in Complexes **2c** and **3**−**5**[a]

| | **2c** (M = Cd) | **3** (M = Fe) | **4** (M = Cd) | **5A**[b] (M = Mg) | **5B**[b] (M = Mg) |
|---|---|---|---|---|---|
| $N_{\text{pyridine}}-M-N_{\text{oxazoline1}}$ | 133.06(18) | 136.89(10) | 131.1(5) | 138.9(2) | 139.4(2) |
| $N_{\text{pyridine}}-M-N_{\text{oxazoline2}}$ | 135.97(19) | 136.89(10) | 137.4(4) | 137.4(2) | 137.4(2) |
| $N_{\text{pyridine}}-M-O_{\text{ether1}}$ | 66.48(16) | 66.92(10) | 68.7(6) | 68.1(2) | 67.83(19) |
| $N_{\text{pyridine}}-M-O_{\text{ether2}}$ | 66.77(17) | 66.47(10) | 64.3(4) | 67.7(2) | 68.00(19) |
| $N_{\text{pyridine}}-M-X_{\text{axial1}}$ | 87.66(14)[c] | 86.02(11)[d] | 86.2(4)[d] | 85.72(19)[d] | 86.55(19)[d] |
| $N_{\text{pyridine}}-M-X_{\text{axial2}}$ | 81.36(18)[c] | 82.98(14)[d] | 84.9(5)[d] | 87.51(19)[d] | 86.48(18)[d] |
| $N_{\text{oxazoline1}}-M-N_{\text{oxazoline2}}$ | 89.64(18) | 86.22(10) | 91.4(4) | 83.67(19) | 83.2(2) |
| $N_{\text{oxazoline1}}-M-O_{\text{ether1}}$ | 151.51(15) | 154.32(10) | 156.2(5) | 151.3(2) | 150.8(2) |
| $N_{\text{oxazoline1}}-M-O_{\text{ether2}}$ | 69.28(15) | 71.75(10) | 69.4(4) | 72.10(19) | 72.26(19) |
| $N_{\text{oxazoline1}}-M-X_{\text{axial1}}$ | 109.24(15)[c] | 98.82(14)[d] | 100.2(5)[d] | 98.19(18)[d] | 98.19(19)[d] |
| $N_{\text{oxazoline1}}-M-X_{\text{axial2}}$ | 81.8(2)[c] | 89.48(15)[d] | 87.0(6)[d] | 86.87(17)[d] | 87.08(18)[d] |
| $N_{\text{oxazoline2}}-M-O_{\text{ether1}}$ | 69.85(17) | 70.68(10) | 69.6(5) | 70.2(2) | 71.07(19) |
| $N_{\text{oxazoline2}}-M-O_{\text{ether2}}$ | 156.97(19) | 153.96(10) | 154.4(3) | 152.7(2) | 151.8(2) |
| $N_{\text{oxazoline2}}-M-X_{\text{axial1}}$ | 86.81(14)[c] | 87.57(12)[d] | 88.0(4)[d] | 87.93(19)[d] | 85.01(18)[d] |
| $N_{\text{oxazoline2}}-M-X_{\text{axial2}}$ | 97.87(18)[c] | 100.26(14)[d] | 97.4(4)[d] | 97.14(19)[d] | 100.22(19)[d] |
| $O_{\text{ether1}}-M-O_{\text{ether2}}$ | 133.14(14) | 133.29(10)[d] | 132.9(5)[d] | 135.8(2)[d] | 135.83(18)[d] |
| $O_{\text{ether1}}-M-X_{\text{axial1}}$ | 89.76(10)[c] | 91.46(10)[d] | 93.6(5)[d] | 92.54(18)[d] | 93.22(18)[d] |
| $O_{\text{ether1}}-M-X_{\text{axial2}}$ | 81.67(17)[c] | 83.94(12)[d] | 81.6(6)[d] | 85.00(17)[d] | 84.21(17)[d] |
| $O_{\text{ether2}}-M-X_{\text{axial1}}$ | 91.41(11)[c] | 82.45(10)[d] | 79.4(3)[d] | 83.44(10)[d] | 84.93(17)[d] |
| $O_{\text{ether2}}-M-X_{\text{axial2}}$ | 88.49(17)[c] | 93.41(12)[d] | 98.3(4)[d] | 93.91(18)[d] | 92.40(17)[d] |
| $X_{\text{axial1}}-M-X_{\text{axial2}}$ | 168.09(13)[c] | 168.99(14)[d] | 170.9(5)[d] | 173.2(2)[d] | 173.0(2)[d] |

[a] Estimated standard deviations are given in parentheses. [b] Two independent cations in the asymmetric unit. [c] $X_{\text{axial1}} = I$, $X_{\text{axial2}} = O_{\text{MeOH}}$. [d] $X_{\text{axial1}} = O_{\text{water1}}$, $X_{\text{axial2}} = O_{\text{water2}}$.

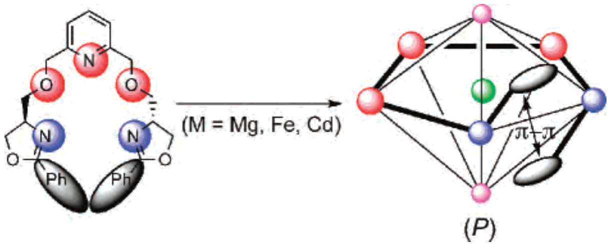

**Figure 6.** Schematic representation of the pentagonal-bipyramidal coordination with (*R*,*R*)-**1**.

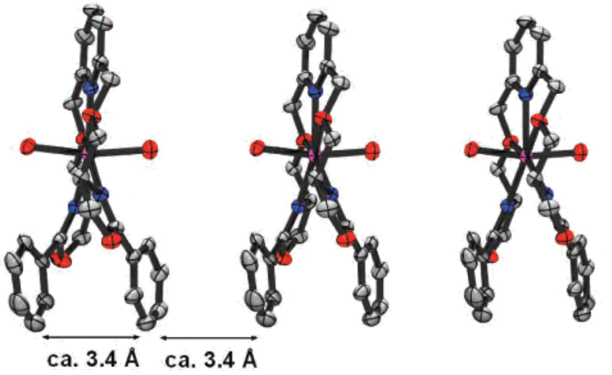

**Figure 7.** Thermal ellipsoid plot of a part of the 1D strand made up by parallel stacking of the cations of **3** (50% probability, hydrogens omitted for clarity). The structures of **4** and **5** are identical with the depicted one.[13]

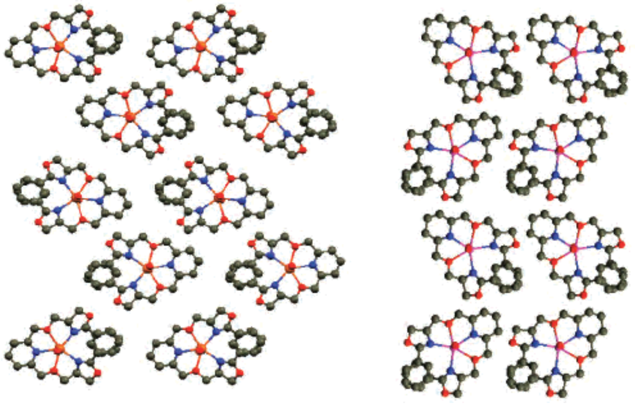

**Figure 8.** View normal to the crystallographic axis *a* (along the one-dimensional columns, only cations shown, hydrogens omitted for clarity) for **3** (left) and **4** (right, identical with **5**).

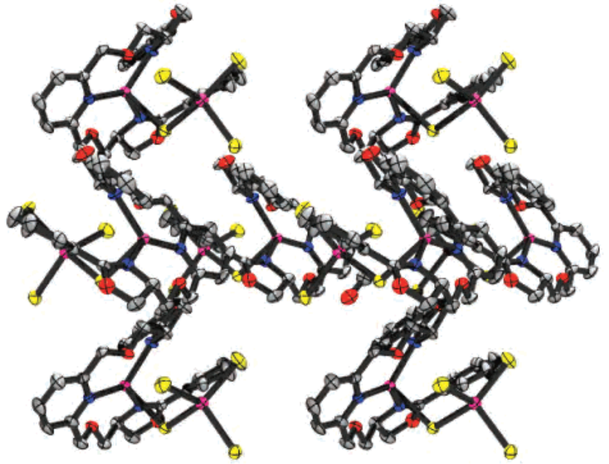

**Figure 9.** Packing diagram for dinuclear complex **2c** (thermal ellipsoid plot, 50% probability, hydrogens and solvent molecules omitted for clarity).

structures are destroyed, yielding $^1$H NMR spectra identical with that of the free ligand. Further evidence for this instability was obtained by growing single crystals from a DMF solution of **2a** through vapor diffusion of $Et_2O$. The X-ray analysis showed the formation of the known compound $[Cd(\mu\text{-}Cl)_2(DMF)_2]_\infty$, also consisting of one-dimensional, chloro-bridged cadmium chains.[20] The solvent of choice for the investigations was $CH_3CN$. For all measurements, both nonrecrystallized bulk material after the initial precipitation and material obtained after recrystallization were used to avoid misinterpretations through crystallization effects. To rule out the existence of slow isomerization processes, the samples were measured twice with an interval of at least 2

---

(20) Linti, G.; Noeth, H.; Thomann, M. *Z. Naturforsch., B: Chem. Sci.* **1990**, *45*, 1463−1471.

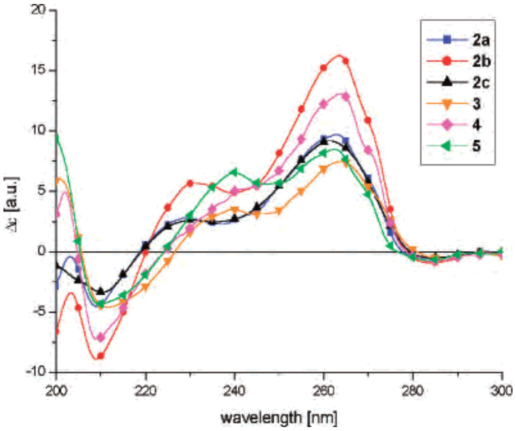

**Figure 10.** CD spectra of compounds **2**−**5** in CH$_3$CN ($c \approx$ with $10^{-4}$ M, 1 mm cylindrical cuvettes).

days. The results were identical in every case showing the stability of the complexes toward degradation in solution and that the complexes investigated initially assembled in solution do not change the coordination geometry upon recrystallization.

Being aware of the limitations to distinguish between monomeric and oligomeric species in solution by mass spectrometry, ESI mass spectrometry gives support that all complex cations are probably mononuclear in CH$_3$CN solution, even for the dinuclear or polymeric species **2a**−**c**. This was concluded from the detection of the cations [M((*R*,*R*)-**1**)]$^{2+}$ or [M((*R*,*R*)-**1**)X]$^{n+}$, and only in the case of **2b** higher aggregates are observed. In addition, for the cadmium halide complexes **2a**−**c** the species [CdX$_3$]$^-$ are the dominating anions.

NMR spectra of the diamagnetic cadmium compounds **2a**−**c** and **4** provided the basis for the assessment of the diastereoselective complex formation in solution. In each case, only one single, $C_2$-symmetrical species could be observed as determined by the number of $^{13}$C signals, with a spectrum distinctively different from the one of the free ligand (*R*,*R*)-**1** (see Supporting Information).[13]

To further investigate the complexes in solution, CD spectra were recorded in CH$_3$CN in the range 200−300 nm (Figure 10). All complexes have UV absorption bands in this region corresponding to n−$\pi$*-transitions starting at approximately 300 nm with peak maxima around 245 nm (**2a**, 247 nm; **2b**, 243 nm; **2c**, 244 nm; **3**, 242 nm; **4**, 243 nm; **5**, 244 nm) on the higher wavelength side of the very intense $\pi$−$\pi$*-bands. Since the free ligand (*R*,*R*)-**1** alone showed no detectable Cotton effects, the appearance of new CD signals can unambiguously be assigned to the corresponding metal complexes.

The CD spectra of **2**−**5** all exhibit a very similar pattern with a positive Cotton effect around 260 nm and a negative one at 210 nm, indicating a very close structural relationship between these complexes. The origin of these bands is probably due to an exiton-coupling between the two phenyl−oxazoline functions,[21] implying close proximity of the two aromatic rings in solution, as it was seen in the crystal structures of **2a**−**c** and **3**−**5**. Therefore, the complex geometry is probably not changed upon dissolving. Together with the fact that all cadmium complexes exist only as one single diasteromer in solution as evidenced by NMR, complete transfer of chirality from the ligand, leading to enantiomerically pure complexes, can be deduced in *all* cases. In addition, the observed CD pattern can be generally regarded as characteristic for a *P*-helical, pentagonal-bipyramidal arrangement of ligand (*R*,*R*)-**1** around divalent metal ions, especially since metal complexes of (*R*,*R*)-**1** with trigonal-bipyramidal geometry show a distinctively different CD pattern.[12b]

## Conclusion

In the course of this investigation, a number of noteworthy results were obtained. We have shown the following: (1) The formation of isostructural inorganic−organic hybrid polymers using CdCl$_2$ or CdBr$_2$[12a] and (*R*,*R*)-**1** is not extendable to CdI$_2$, yielding only the dinuclear complex **2c**. (2) With noncoordinating perchlorate anions, Fe(II), Cd(II), and Mg(II) form pentagonal-bipyramidal complexes, extending the set of suitable metal ions for pentagonal-bipyramidal geometry with ligand (*R*,*R*)-**1**. (3) All complexes described here exhibit an unprecedented *P*-helical arrangement of ligand (*R*,*R*)-**1** in the pentagonal plane in the solid as well as the solution state. (4) The pentagonal bipyramid is likely to be stabilized by $\pi$−$\pi$-stacking of the phenyl rings. This could constitute a new approach toward this coordination geometry in comparison to the commonly encountered stabilization by macrocyclic or resonance-stabilized ligands. (5) Not only the polymeric cadmium halide complexes but also the mononuclear species show columnar stacking in the solid state, stabilized by intermolecular $\pi$−$\pi$-interactions, yielding highly ordered, supramolecular helicity in one single direction in space. (6) All complexes show very characteristic CD bands in solution. The pattern is assigned to a *P*-helical, pentagonal arrangement of the ligand around divalent cations.

## Experimental Section

**General Remarks.** *Caution: Although no accident was observed handling the compounds described below, perchlorate salts should be regarded as potentially explosive and handled with care!* Reactions were carried out under a dry, oxygen-free atmosphere of N$_2$ in flame-dried Schlenk glassware where indicated. Commercially available reagents were used as received. CH$_3$CN was distilled over P$_4$O$_{10}$. THF and Et$_2$O were dried with Na/benzophenone and stored over Na wire. MeOH was dried with Mg/I$_2$ and stored over molecular sieves 3 Å. NMR spectra were recorded on Bruker Avance 300 ($^1$H, 300 MHz; $^{13}$C, 75.5 MHz). X-ray analysis was performed by the Crystallography Laboratory (University of Regensburg, S.S., M.Z.). Elemental analysis (Heraeus elementar vario EL III) and mass spectrometry (Finnigan ThermoQuest TSQ 7000) were done by the Central Analytical Laboratory (University of Regensburg). CD spectra were recorded on a Jasco J-710 spectropolarimenter using CH$_3$CN solutions (HPLC grade) in cylindrical 1 mm cuvettes.

**(*P*)-[Cd((*R*,*R*)-1)($\mu$-Cl)$_2$CdCl$_2$]$_\infty$ (2a).**[12a] Under N$_2$ a mixture of 319 mg (1.58 mmol, 1.0 equiv) of CdCl$_2$·H$_2$O and 725 mg (1.58

---

(21) Ziegler, M.; Von Zelewsky, A. *Coord. Chem. Rev.* **1998**, *177*, 257−300.

mmol, 1.0 equiv) of **1** in 20 mL of dry MeOH was refluxed for 3 h. After the sample was cooled to ambient temperature, the formed white precipitate was collected, washed with cold dry MeOH, and dried in vacuo to yield 368 mg (57%) of a colorless solid. Crystals suitable for X-ray analysis were obtained by diffusion of $Et_2O$ into a solution of **2a** in $CH_3CN$. (Note: the title compound was only sparingly soluble in $CH_3CN$. Therefore no $^{13}C$ NMR could be obtained.)

Mp: >200 °C. $^1H$ NMR (300 MHz, $CD_3CN$): $\delta = 7.94$ (t, $J = 7.8$ Hz, 1 H), 7.75−7.59 (m, 4 H), 7.53−7.17 (m, 8 H), 5.10−4.87 (m, 6 H), 4.64 (dd, $J = 10.4$, 9.1 Hz, 2 H), 4.20−4.04 (m, 4 H), 3.73 (dd, $J = 11.0$, 8.5 Hz, 2 H). $^1H$ NMR (300 MHz, $CD_3CN$): solubility too low. MS (ESI, $CH_3CN$): *m/z* (%) = 458.1 (58, [(*R*,*R*)-**1**]$^+$), 606.1 (100, [Cd((*R*,*R*)-**1**)Cl]$^+$). MS (-ESI, $CH_3CN$): *m/z* (%) = 218.3 (100, [$CdCl_3$]$^-$). Anal. Calcd for $C_{27}H_{27}Cd_2Cl_4N_3O_4$ ($M_r$ = 824.14): C, 39.35; H, 3.30; N, 5.10. Found: C, 39.35; H, 3.40; N, 5.17.

**(*P*)-[Cd((*R*,*R*)-1)($\mu$-Br)$_2$CdBr$_2$]$_\infty$ (2b).**[12a] Under $N_2$ a mixture of 344 mg (1.26 mmol, 1.0 equiv) of $CdBr_2$ and 578 mg (1.26 mmol, 1.0 equiv) of **1** in 10 mL of dry MeOH was refluxed for 1 h. After the sample was cooled to ambient temperature, the white solid was collected, washed with dry, cold MEOH, and dried in vacuo to yield 478 mg (76%) of a colorless solid. Crystals suitable for X-ray analysis were obtained by diffusion of $Et_2O$ into a solution of **2b** in $CH_3CN$.

Mp: >200 °C. $^1H$ NMR (300 MHz, $CD_3CN$): $\delta = 7.95$ (t, $J = 7.9$ Hz, 1 H), 7.75−7.59 (m, 4 H), 7.54−7.43 (m, 2 H), 7.38 (d, $J = 7.9$ Hz, 2 H), 7.33−7.20 (m, 4 H), 5.08−4.87 (m, 6 H), 4.65 (dd, $J = 10.4$, 9.1 Hz, 2 H), 4.22−4.05 (m, 4 H), 3.76 (dd, $J = 11.0$, 8.5 Hz, 2 H). $^{13}C$ NMR (75.5 MHz, $CD_3CN$): $\delta = 169.2$, 155.2, 140.3, 133.5, 130.3, 128.7, 126.2, 122.7, 73.6, 70.7, 70.1, 66.2. MS (ESI, $CH_3CN$): *m/z* (%) = 458.1 (46, [**1**]$^+$), 480.1 (100, [Na(**1**)]$^+$), 558.1 (11, [$Cd_3Br_4$(**1**)]$^{2+}$), 594.1 (6), 650.0 (5, [Cd(**1**)Br]$^+$). MS (-ESI, $CH_3CN$): *m/z* (%) = 440.4 (100). Anal. Calcd for $C_{27}H_{27}Br_4Cd_2N_3O_4$ ($M_r$ = 1001.94): C, 32.37; H, 2.72; N, 4.19. Found: C, 32.37; H, 2.61; N, 4.56.

**(*P*)-[Cd((*R*,*R*)-1)(MeOH)($\mu$-I)CdI$_3$]·MeOH (2c).** Under $N_2$ a mixture of 197 mg (539 $\mu$mol, 2.0 equiv) of $CdI_2$ and 123 mg (269 $\mu$mol, 1.0 equiv) of (*R*,*R*)-**1** in 5 mL of dry MeOH was refluxed for 1 h and filtered hot. The resulting precipitate was redissolved by heating to reflux, and the solution was slowly tempered to ambient temperature in the course of ca. 1 h. A total of 317 mg (94%) of block-shaped colorless crystals suitable for X-ray analyses was obtained.

Mp: 131−137 °C. $^1H$ NMR (300 MHz, $CD_3CN$): $\delta = 7.97$ (t, $J = 7.8$ Hz, 1 H), 7.72−7.58 (m, 4 H), 7.57−7.45 (m, 2 H), 7.44−7.25 (m, 6 H), 5.02−4.84 (m, 6 H), 4.65 (dd, $J = 10.2$, 9.1 Hz, 2 H), 4.23−4.07 (m, 4 H), 3.78 (dd, $J = 10.8$, 8.6 Hz, 2 H). $^{13}C$ NMR (75.5 MHz, $CD_3CN$): $\delta = 169.5$, 155.1, 140.6, 133.7, 130.3, 128.9, 126.2, 122.9, 73.5, 70.4, 70.3, 66.0. MS (ESI, $CH_3CN$): *m/z* (%) = 458.1 (100, [(*R*,*R*)-**1**]$^+$), 480.1 (5, [Na((*R*,*R*)-**1**)]$^+$), 698.1 (24, [Cd((*R*,*R*)-**1**)I]$^+$). MS (-ESI, $CH_3CN$): *m/z* (%) = 494.5 (100, [$CdI_3$]$^-$). Anal. Calcd for $C_{29}H_{35}Cd_2I_4N_3O_6$ ($M_r$ = 1254.04): C, 27.77; H, 2.81; N, 40.48. Found: C, 27.82; H, 3.03; N, 40.33.

**(*P*)-[Fe((*R*,*R*)-1)(H$_2$O)$_2$](ClO$_4$)$_2$·THF (3).** Under $N_2$ 51.2 mg (141 $\mu$mol, 1.0 equiv) of $Fe(ClO_4)_2 \cdot 6H_2O$ and 64.5 mg (141 $\mu$mol, 1.0 equiv) of (*R*,*R*)-**1** were dissolved separately in 5 mL of dry THF each. The ligand solution was transferred to the metal salt. A small amount of a brown oil separated almost immediately. The supernatant solution was decanted and left overnight without stirring at ambient temperature. A colorless solid separated and was collected on a membrane filter (Schleicher & Schuell, RC-L 58, 0.2 $\mu$m), washed with $Et_2O$, and dried in vacuo to yield 50 mg (43%) of colorless needles, which were suitable for X-ray diffraction. Alternatively, crystals can be grown by slow vapor diffusion of $Et_2O$ into a solution of **3** in $CH_3CN$.

Mp: 117−119 °C (dec). MS (ESI, $CH_3CN$): *m/z* (%) = 256.4 (17, [Fe((*R*,*R*)-**1**)]$^{2+}$), 458.1 (100, [H**1**]$^+$). Anal. Calcd for $C_{31}H_{39}Cl_2FeN_3O_{15}$ ($M_r$ = 820.40): C, 45.38; H, 4.79; N, 5.12. Found: C, 45.20; H, 4.70; N, 5.02.

**(*P*)-[Cd((*R*,*R*)-1)(H$_2$O)$_2$](ClO$_4$)$_2$·*x* solv (4).** Under $N_2$ 233 mg (555 $\mu$mol, 1.0 equiv) of $Cd(ClO_4)_2 \cdot 6H_2O$ and 254 mg (555 $\mu$mol, 1.0 equiv) of **1** were dissolved separately in 10 mL of dry THF each. The ligand solution was transferred to the metal salt. Precipitation of the complex started immediately upon addition. The mixture was stirred at ambient temperature for 1 h. The precipitate was collected on a membrane filter (Schleicher & Schuell, RC-L 58, 0.2 $\mu$m), washed with THF and $Et_2O$, and dried in vacuo to yield 427 mg of a colorless solid. Crystals suitable for X-ray analysis could be obtained by slow vapor diffusion of $Et_2O$ into a solution of **4** in $CH_3CN$.

Mp: >200 °C. $^1H$ NMR (300 MHz, $CD_3CN$): $\delta = 8.02$ (t, $J = 7.8$ Hz, 1 H), 7.62−7.50 (m, 2 H), 7.48−7.30 (m, 10 H), 5.10−4.85 (m, 6 H), 4.69 (dd, $J = 10.4$, 9.3 Hz, 2 H), 4.29−4.15 (m, 4 H), 3.81 (dd, $J = 11.1$, 8.4 Hz, 2 H), 3.69−3.55 (m, 4 H, THF), 1.85−1.72 (m, 4 H, THF). $^{13}C$ NMR (75.5 MHz, $CD_3CN$): $\delta = 170.5$, 154.9, 140.8, 134.1, 129.8, 129.1, 125.7, 122.8, 73.2, 70.4, 70.3, 68.4, 65.9, 26.3. MS (ESI, $CH_3CN$): *m/z* (%) = 285.0 (80, [Cd((*R*,*R*)-**1**)]$^{2+}$), 305.6 (100, [Cd((*R*,*R*)-**1**)($CH_3CN$)]$^{2+}$), 458.1 (37, [H**1**]$^+$), 670.1 (13, [Cd((*R*,*R*)-**1**)($ClO_4$)]$^+$).

**(*P*)-[Mg((*R*,*R*)-1)(H$_2$O)$_2$](ClO$_4$)$_2$·*x* solv (5).** Under $N_2$ 267 mg (1.20 mmol, 1.0 equiv) of $Mg(ClO_4)_2 \cdot xH_2O$ and 547 mg (1.20 mmol, 1.0 equiv) of **1** were dissolved separately in 10 mL of dry THF each. The ligand solution was transferred to the metal salt. The solution was stirred at ambient temperature for 4 h, before the solvent was removed in vacuo. The slightly yellow residue was treated with 20 mL of dry $Et_2O$, and the suspension was stirred vigorously for 1 h. The solid was collected, washed with dry $Et_2O$, and dried under reduced pressure to yield a slightly yellow solid (596 mg). Crystals suitable for X-ray analysis could be obtained by slow vapor diffusion of $Et_2O$ into a solution of **5** in acetone.

Mp: 110−123 °C (dec). MS (ESI, $CH_3CN$): *m/z* (%) = 240.5 (37, [Mg((*R*,*R*)-**1**)]$^{2+}$), 261.0 (100, [Mg((*R*,*R*)-**1**)($CH_3CN$)]$^{2+}$), 458.1 (83, [H((*R*,*R*)-**1**]$^+$), 580.1 (15, [Mg((*R*,*R*)-**1**)($ClO_4$)]$^+$).

**Acknowledgment.** This work was supported by the German Research Foundation (DFG) as part of the program SP1118 (RE948/5-2) and the Fonds der Chemischen Industrie (Ph.D. fellowship to A.K. and Forschungsbeihilfe).

**Supporting Information Available:** Extended X-ray crystallographic data and CIF files for **2c**−**5** and NMR spectra for (*R*,*R*)-**1**, **2c**, and **4**. This material is available free of charge via the Internet at http://pubs.acs.org.

IC050014B